IJCPS Vol. 11, No. 4, Jul-Aug 2022
www.ijcps.org
DOI Prefix:10.30731/ijcps

International Journal of Chemical and Physical Sciences
(Peer-Reviewed Journal)
ISSN:2319-6602

Exploration of the efficacy of a novel copper (II) complex as a potential anti-COVID agent

Amarjit Kamath[1], Dipu Kumar Mishra[1], Anmol Chettri[1], Indrani Sarkar[2], Debadrita Roy[1], Indrajit Barman[1], Vikas Kumar Dakua[3], Arnab Sen[2] and Biswajit Sinha[1]*

[1]Department of Chemistry, University of North Bengal, Darjeeling, India
[2]Molecular Genetics Laboratory, Department of Botany, University of North Bengal, India
[2]Department of Chemistry, Alipurduar University, Alipurduar, India

***Corresponding Author E-Mail:** biswachem@gmail.com

Abstract

Metal-organic hybrid complexes of copper can act as potential antibacterial, anti-fungal, anti-viral agents owing to their fascinating structures and biocompatibility. Hence a novel Copper (II) complex entitled as [{Diaquo(3,5-dinitrobenzoato-κ^1O^1)(1,10-phenanthroline-$\kappa^2N^1:N^{10}$)}copper(II)]3,5-dinitrobenzoate synthesized earlier following hydrothermal method was examined for its efficacy as a potential anti-COVID agent. The complex has a distorted square pyramidal geometry and crystallizes with the space group $P12_11$ (monoclinic). The pharmokinetic property of the complex was assessed by using pkCSM server. The physicochemical properties, lipophilicity, drug likeliness and medicinal properties were also explored theoretically. Molecular docking and simulation studies proved its potential binding affinity with SARS-COV2 spike protein. Low gastrointestinal absorption (GI) and good skin permeation of the complex suggest that the complex may be potentially a good candidate for injection against COVID-19 infections.

Keywords: *Hydrothermal synthesis, Single crystals, Molecular docking, SARS-COV-2, Pharmacokinetics.*

Introduction:

The latest threat to global health is the ongoing Severe Acute Respiratory Syndrome- Corona Virus 2(SARS-CoV2).[1] This virus emerged at the latter half of 2019 in Wuhan, China. Within very short time it spread to almost every continent except Antarctica and became a pandemic after H1N1 Swine Flu pandemic in 2009-2010.[2] In India, total count of infected victims has risen to about 16.3 million with more than three lakh of new cases reporting every day since the inception of the second wave.[3] Around 187K people have lost their lives in India till date and the fatalities are counting significantly each day.[3] The situation is becoming worse every single day and human beings, the most advanced creation of nature, is still trying hard to solve the puzzle and save mankind from this lethal single-stranded RNA virus.[4] Hence governments of all countries have imposed several measures to combat the situation like social distancing, complete lockdown, wearing face mask and gloves, using alcohol based sanitizers, *etc*., to common people for controlling the spread of infection by this highly contagious virus. Although these measures have served their purpose to some extent, they are not at all sufficient measures to control the present pandemic situation.

A combination of azithromycin and hydroxychloroquine has been used primarily for the treatment of the disease.[5] Research on COVID-19 have shown that the human to human as well as cross species transmission of the virus is chiefly regulated by the spike protein receptor binding domain and its

host receptor (ACE2) as similar to SARS-CoV outbreak in 2002.[5] The viral genome encrypts various non-structural proteins and structural proteins that play pivotal roles in binding the virus to host cellular receptors and thereby regulates viral replication and thus facilitates subsequent infection.[7,8] The presence of prominent spike (S) protein on its surface helps in viral attachment and its successful fusion into the host cells.[9] The imperative main protease enzyme Mpro (also referred to as 3 C-like protease) of SARS-CoV-2 plays pivotal role in proteolytic cleavage and processing of the large viral polyprotein orf1ab in combination with papain-like proteases and facilitates viral replication.[10-12] The anti-malarial drug, hydroxychloroquine (HCQ), promotes endosomal acidification and blocks the entry of the virus by inhibiting glycosylation of the cellular receptors responsible for binding with viral proteins.[13] Thus HCQ was observed to be very effective against viral growth but the major drawback in its use was drug poisoning and severe toxic side effects.[14] The other antiviral drugs, *viz.*, Favipiravir and Remdesivir can inhibit the RdRp activity and control the replication of SARS-COV2 virus under clinical trial.[15,16] The relentless attempts of the medical practitioners and researchers across the world could not yet find an effective/specific remedy to culminate the infectious transmission and the calamitous health disaster posed by highly intimidating SARS-CoV-2. Though several drugs and vaccines are in clinical trials all over the world, an effective therapeutic remedy specifically targeted to treat and cure COVID-19 is yet to be achieved or invented. Researchers working in bioinorganic chemistry field, often find copper complexes as novel metallodrugs with stronger efficacies in therapeutic applications.[17] Copper complexes with some bioactive ligands like 1,10-phenanthroline or its derivatives or heterocyclic ligands with nitrogen atoms have been the area of interest over the years. Cu-phenanthroline complexes add new dimension to the design and development of molecules that can tune metal-toxicity.[18,19] Therefore, the potential use of copper complexes as antiviral, anti-inflammatory, antimicrobial, antitumor agents, chemical nucleases or enzyme inhibitors attracts the attention of researchers from various parts of the world. Markedly, the biochemical action of Cu(II) complexes with non-steroidal anti-inflammatory drugs (NSAIDs) has been studied recently.[20] For instance, the infectivity of influenza virus gets reduced significantly when exposed to copper surfaces.[21] It was speculated that the viral nucleic acid undergoes degradation due to the intervention of copper(II) ions. In addition, the study and development of Cu complexes could be helpful in the design and production of antiviral and antibacterial materials that may be able to deactivate HIV or H1N1 viruses[22] and antibiotic-resistant bacteria, respectively. Research is going on for repurposing of already approved and available drugs against Covid-19. Molecular simulation and molecular dynamics simulation have been proved to be a good measure to identify potential small molecules which can target Covid-19 proteins with maximum capacity.[10] Therefore, herein this work a hydrothermally synthesized Cu(II) complex, [{Diaquo(3,5-dinitrobenzoato-κ^1O^1)(1,10-phenanthroline-κ^2N^1:N^{10})}copper(II)] 3,5-dinitrobenzoate, was examined to explore its potency as a potential anti-covid agent through molecular docking and ADMET property studies against SARS-COV2 virus.

Experimental:

Materials and Methods

The Cu(II) complex was synthesized by following hydrothermal method under autogenous pressure in a 10 mL Teflon-lined stainless steel autoclave at 150 °C. $Cu(NO_3)_2{\cdot}2H_2O$ (99 %), 1,10-phenanthroline (99 %) abbreviated as phen, 3,5-dinitrobenzoic acid (98.5 %) abbreviated as Hdnb and de-ionized water (with specific conductance < $1{\cdot}10^{-6}$ $S{\cdot}cm^{-1}$ at 25 °C) were used in this synthesis. All the analytical grade chemicals were procured from S. D. Fine Chemicals, India. Oxford diffractometer fitted

with CCD camera was used for Single crystal X-ray diffraction study. PAN analytical X′pert powder X-ray diffractometer used for powder X-ray diffraction (PXRD) to check purity and the homogeneity of the bulk complex. The crystal morphology was studied using Field Emission Scanning Electron Microscopy (FESEM, INSPECT F50, FEI, The Netherland). Elemental micro-analyses (C, H and N) were carried out using Perkin–Elmer (Model 240C) analyzer. Cu-content was determined with the aid of AAS (Varian, SpectrAA 50B) by using standard Cu-solution from Sigma-Aldrich, Germany.

Synthesis of the copper complex

A mixture of $Cu(NO_3)_2{\cdot}2H_2O$ (0.2416 g), 1,10-phenanthroline (0.1982 g) and 3,5-dinitrobenzoic acid (0.2120 g) was minced with an agate mortar and pastle. The mixture was then filled in a 10 mL Teflon tube and de-ionized water (4.0 mL) was added. The mixture was stirred for about 30 minutes to obtain homogeneous suspension. Then the loaded tube was packed in stainless steel autoclave and heated at 150 °C in an automated hot-air oven for about 48 h. The autoclave was allowed to natural cooling at room temperature. The reaction mixture was then filtered, washed successively with ethanol and de-ionized water. The blue colored solid residue was left for air-drying for several hours. Yield: 0.456 g (70 % based on copper). Blue needle shaped single crystals appropriate for single crystal X-ray diffraction study was handpicked under a microscope (40X). Elemental analysis: calcd (%) for $[Cu(C_7H_3N_2O_6)(C_{12}H_8N_2)(H_2O)_2](C_7H_3N_2O_6)$: C, 44.48; H, 2.58; N, 11.97; Cu, 9.05 and found: C, 44.45; H, 2.56; N, 11.89; Cu, 8.86.

X-ray Crystal Structure determination

Single crystal X-ray diffraction data were collected on an Oxford diffractometer (with Mo *K*α, wavelength = 0.71 Å) equipped with CCD camera and an Oxford Cryosystem open-flow nitrogen cryostat with a normal stability of 0.1 K. An absorption multiscan or analytical correction[23] was applied to all the data and analyzed with related softwares.[24] SIR97 program in combination with Fourier difference synthesis was used to resolve the structure of the complex.[25] The structure was refined against *F* or *F2* using CRYSTAL program.[26] All the H-atoms were located in a difference Fourier map but those attached to C-atoms were repositioned geometrically. The H-atoms were initially refined with soft constraints on the bond lengths (C-H = 0.93-0.98, N-H 0.86-0.89 and O-H = 0.82 Å) and angles to regularize their geometry with U_{iso} (H) in the range 1.2-1.5 times U_{eq} of the parent atom and the corresponding positions were refined with a riding constraints.[27] All non-hydrogen atoms were refined with anisotropic displacement parameters. Pertinent crystal parameters and structure refinement of the complex are summarized in Table I-S and selected bond lengths and angles are listed in Table II-S.

Preparation of Receptor Protein

Structure of SARS-CoV-2 spike receptor with PDB Id: 7BZ5 was obtained from Protein data bank (PDB). This structure was also used by other researches as a target protein for drug repurposing studies supporting its ideal candidature. The protein was prepared for docking studies after deletion of the water molecules and addition of polar Hydrogens. Non-Polar hydrogens were merged with polar hydrogens. Gasteiger charge of -3.6 was added to the protein. Finally the pdb format of the receptor was changed to pdbqt and it was used for the docking studies.

Ligand structure preparation

The complex, [{Diaquo(3,5-dinitrobenzoato-κ^1O^1)(1,10-phenanthroline-κ^2N^1:N^{10})}copper(II)] 3,5-dinitrobenzoate, examined in this study was synthesized earlier following hydrothermal method.[28] Its chemical structure was prepared first in .mol format. Smiles server converted the .mol to .sdf and

subsequently, .sdf to .pdb format. The .pdb structure was converted into .pdbqt after opting torsion angles and categorizing the rotatable bonds present within them.

Molecular docking and dynamics study

Molecular docking was done by Autodock version 4.[29] Since the compound contained a metal ion, *i.e*., copper(II) ion, Autodock vina was not employed. Since this is a novel compound there was uncertainty whether the popular docking sites of the 6LU7 will be the best binding site for this molecule. Hence one cycle of blind docking was preferred to get an idea about the best binding sites and then targeted the specific site for next cycle of docking. This strategy worked well for two advantages: i) firstly the blind docking provided the opportunity to identify all the possible sites wherein the new compound can bind irrespective of all the binding sites reported so far. Thus the result was completely unbiased, and ii) secondly a new target site was found. A number of studies involving the docking of proposed drugs at the active site of Covid-19 protein were intentionally performed, because such proteins interact with the human receptor. However, the strategy followed herein this study identified some allosteric sites that are completely different from active sites. Inhibition of these allosteric sites may prove to be beneficial in inactivating the active site itself. Investigation on atomic behavior, conformational changes at atomic level and structural constancy of a protein through molecular dynamic (MD) simulation has become a popular method in protein-ligand complex study. The docked complex was subjected to MD simulation by Gromacs [30] using Gromacs96 53a6 force field. The temperature was set to 303 K. MD simulations were performed for 100 ns time scale, with 10,000 steps of energy minimization through steepest descent mechanism.

Determination of ADMET properties of the ligand

Pharmacokinetic studies furnish information regarding drug concentrations in various parts of an organism with respect to time. The drugs, administered into the body of an organism, require passing through several biological barriers. Thus, the major properties like absorption, distribution, metabolism and excretion (*i.e*, ADME) are crucial parameters for any compound to be established as a drug and therefore a priori clinical and animal studies it is mandatory to explore their pharmacokinetic properties.[31] The properties for instance lipophilicity ($LogP_{o/w}$), water soluble ability (LogS), gastrointestinal absorption (GI), Blood - Brain Barrier (BBB) and CYP1A2 inhibitor are very important pharmacokinetic parameters for any compound.[32] Therefore, the pharmacokinetic properties such as lipophilicity ($LogP_{o/w}$), water soluble ability (LogS), gastrointestinal absorption (GI), Blood-Brain Barrier (BBB) and CYP1A2 inhibitor of the complex were determined to ascertain its drug likeliness character using Swiss ADME. Swiss ADME[33] was used for characterizing the complex used as ligand in this study in term of properties like lipophilicity, water solubility, Pharmacokinetics, drug likeliness and medicinal protertiesy. A pharmacokinetic property of this complexwas further assessed with pkCSM server.[34]

Results And Discussion

Structural Description and properties of the complex

Single crystal X-ray diffraction analysis of the synthesized complex, [{Diaquo(3,5-dinitrobenzoato-κ^1O^1)(1,10-phenanthroline-κ^2N^1:N^{10})}copper(II)]3,5-dinitrobenzoate, *[Cu(dnb)(phen)-$(H_2O)_2$]·(dnb)*,[35] revealed that it crystallizes in a monoclinic form with space group $P12_11$ (Table I-S).

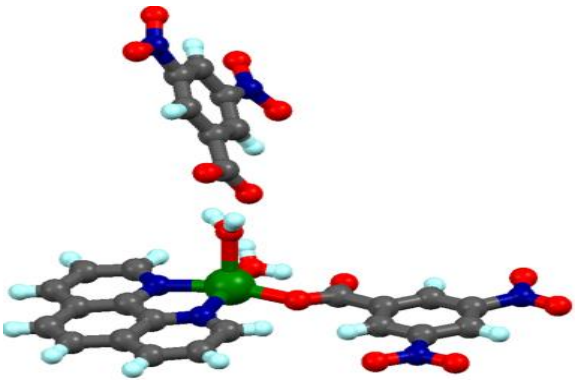

Fig. 1. The asymmetric unit of the complex (Color: Green, Cu; Blue, N; Red, O; Grey, C; Sky Blue, H).

The asymmetric unit comprises of a Cu(II) ion coordinated to two N-atoms of phen simultaneously, two O-atoms of two water molecules, one O-atom of dnb^- moiety and a non-coordinated dnb^- moiety as counter anion as portrayed in Fig. 1. It is quite apparent that Cu(II) ion is penta-coordinated with a distorted square pyramidal geometry. The bond length between Cu1 and O-atoms of two coordinated H_2O molecules are Cu1-O2 = 1.957 Å (water molecule located in the molecular plane) and Cu1-O3 = 2.198 Å (water molecule located above molecular plane). The other bond distances and angles of the coordination sphere are summarized in Table II-S. The steric hindrance existing between the phen ligands and dnb- moieties leads to the distortion in the geometry of the complex. A dihedral angle of 5.73° was observed due to this steric repulsion.[35-37] The Cu(II) ion is seen to be positioned 0.474 Å above the plane of square pyramid. The distortion in the geometry of the complex was well supported by Addison parameter, τ {τ = (β-α)/60} value.[38] The τ value for a square bipyramidal and a trigonal bipyramidal are 0 and 1.0, respectively. Addison parameter of the complex was found to be 0.11, supporting it's distorted square pyramidal geometry. The selected hydrogen-bond geometry of the complex is summarized in Table III-S. The H-atoms of the coordinated axial water molecule are engaged in inter-molecular hydrogen bonding with two adjacent dnb^- moieties, while the H-atoms of the coordinated equatorial water molecule are involved in both inter and intra-molecular hydrogen bonding (Fig. 1-S) with coordinated and non-coordinated dnb^- moieties, respectively. The large-scale hydrogen bonding helped the complex to achieve a three-dimensional structure and stability.

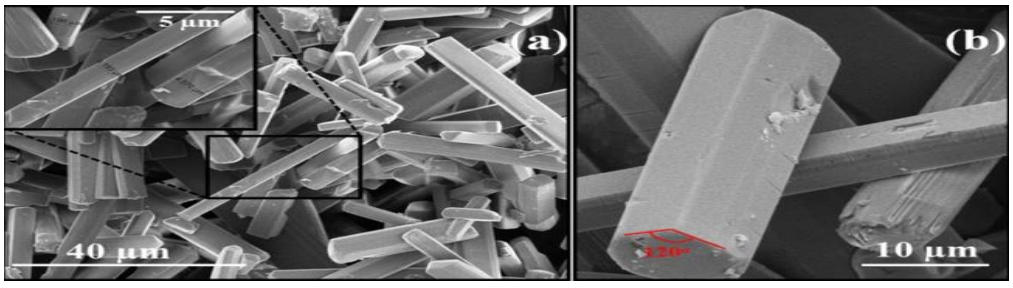

Fig. 2. FESEM images of the crystal: (a) the average cross section of the crystals around 3-5 μm and (b) its hexagonal cross section.

The phase purity was confirmed through powder X-ray diffraction studies. The simulated and experimental X-ray diffraction (PXRD) patterns obtained at room temperature are shown in Fig. 2-S. They are more or less similar to each other and conforms the purity of the single crystals to be the

representative of the bulk samples. Morphological study of the crystals with FESEM (Fig. 2) reveals that the crystals are rod shaped and have well characterized regular faces with thickness of 3-4 μm and lengths up to 60 μm. The other properties like magnetic property and Hirschfeld surface analysis of the crystal have already reported by Kamath *et. al*.[28]

Molecular docking studies

The blind docking predicted nine potential sites wherein the considered ligand can bind. Amongst them the most suitable site was composed of Thr85 (L), Lys 39(L), Lys 42(L), GLN39 (H), Tyr 94(H), Gly42 (H), Ala 40(H) and Lys43 (H) and it was evident that the best binding sites constituted of more than one chain and they were H and L. The blind docking revealed an affinity of -8.4 kcal/mol. When the site specific docking was performed the value was raised to -8.7 kcal/mol (Fig. 3).

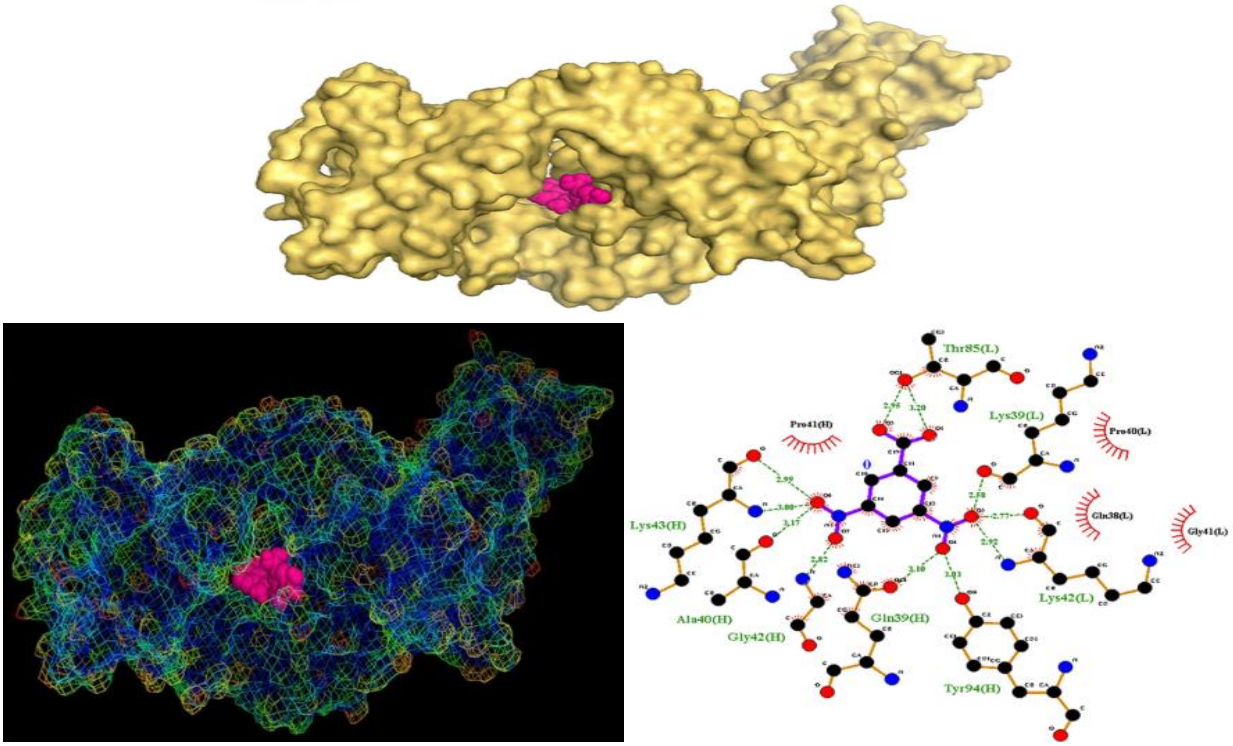

Fig. 3. The site-specific binding affinity of the ligand with Covid-19 protease (PDB Id: 7BZ5) and interacting amino acids.

Various parameters obtained from the pharmacokinetic (ADME) studies of the complex were listed in the Table I. The ADME study of the selected compound revealed that the molecular weight of this ligand was 739.29 g/mol. Moreover, the number of hydrogen donor and acceptor were more than 5 (13 and 20, respectively). Thus, it was evident that this compound does not obey the Lipinski's rule of five and it is thus not a good candidate to be administered orally to human beings. However, the $LogK_p$ (skin permeation) value was found to be -11.73 cm/s suggesting its fine skin permeability.[39] Hence, it can hypothesized that this compound, although cannot be administered orally as drug, it has sufficient quality to be administered as injection either subcutaneous or intradermally as far as the $LogK_p$ value is concerned. It's a well known fact that subcutaneous administration speeds up the movement of the drug to the local lymph node to elicit its response.[40] Orally administered drugs are good for local response, however, the subcutaneous or intradermal administration is better when fighting against a virus affecting

more than one physiological system.[40] Another major advantage of subcutaneous administration is its favorability for consistent delivery with lower volume.[40] Since the GI absorption of the complex is considerably low and skin permeation is good, this complex may be a good candidate for injection against Covid-19.

Root-mean square deviation

To investigate the variations in the molecular dynamics of protein along with the conformational stability of the protein-ligand complex, *RMSD* values of the protein (7BZ5) and ligand-docked protein were compared. The C-alpha atom *RMSD* values were plotted against time. *RMSD* for 7BZ5 varied approximately from 1.4 to 3.3, whereas the corresponding values ranged from 1.2 to 2.3 for the docked complex (Fig. 4). Lower *RMSD* values of the docked complex than the single protein proposes the conformational stability of the protein-ligand complex.

Table 1: Pharmacokinetic (ADME) properties of the Cu(II) complex.

Properties	Predicted values
Molecular Weight	739.29
Heavy atoms	47
Aromatic heavy atoms	0
Fraction Csp3	1
Rotatable bonds	8
H-bond acceptors	20
H-bond donors	13
MR	159.29
TPSA	269.66
iLOGP	0
XLOGP3	-1.3
WLOGP	-0.54
MLOGP	-2.57
Silicos-IT LogP	-5.04
Consensus LogP	-1.89
ESOL LogS	-3.08
ESOL Solubility (mg/mL)	0.62
ESOL Solubility (mol/L)	0.000838
ESOL Class	Soluble
Ali Log S	-3.87
Ali Solubility (mg/mL)	0.101
Ali Solubility (mol/L)	0.000136
Ali Class	Soluble
Silicos-IT LogSw	2.42
Silicos-IT Solubility (mg/mL)	194000
Silicos-IT Solubility (mol/L)	262
Silicos-IT class	Soluble

GI absorption	Low
BBB permeant	No
Pgp substrate	Yes
CYP1A2 inhibitor	No
CYP2C19 inhibitor	No
CYP2C9 inhibitor	Yes
CYP2D6 inhibitor	No
CYP3A4 inhibitor	No
log Kp (cm/s)	-11.73
Lipinski violations	3
Ghose violations	4
Veber violations	1
Egan violations	1
Muegge violations	4
Bioavailability Score	0.17
PAINS alerts	0
Brenk alerts	2
Leadlikeness violations	2
Synthetic Accessibility	7.71

Root mean square fluctuation

RMSF values for C-alpha atoms of each amino acid of the receptor protein was calculated and plotted against the number of residues. This plot revealed similar pattern of residue-fluctuation for both 7BZ5 and the docked complex (Fig. 4). *RMSF* analysis clearly indicated that binding of the investigated ligands to the Covid spike protein raised no major complications in terms of protein flexibility and structural conformations.

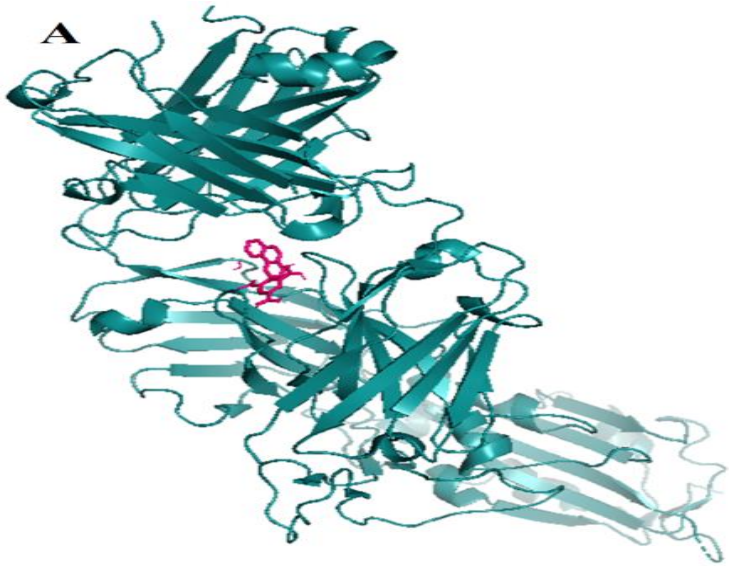

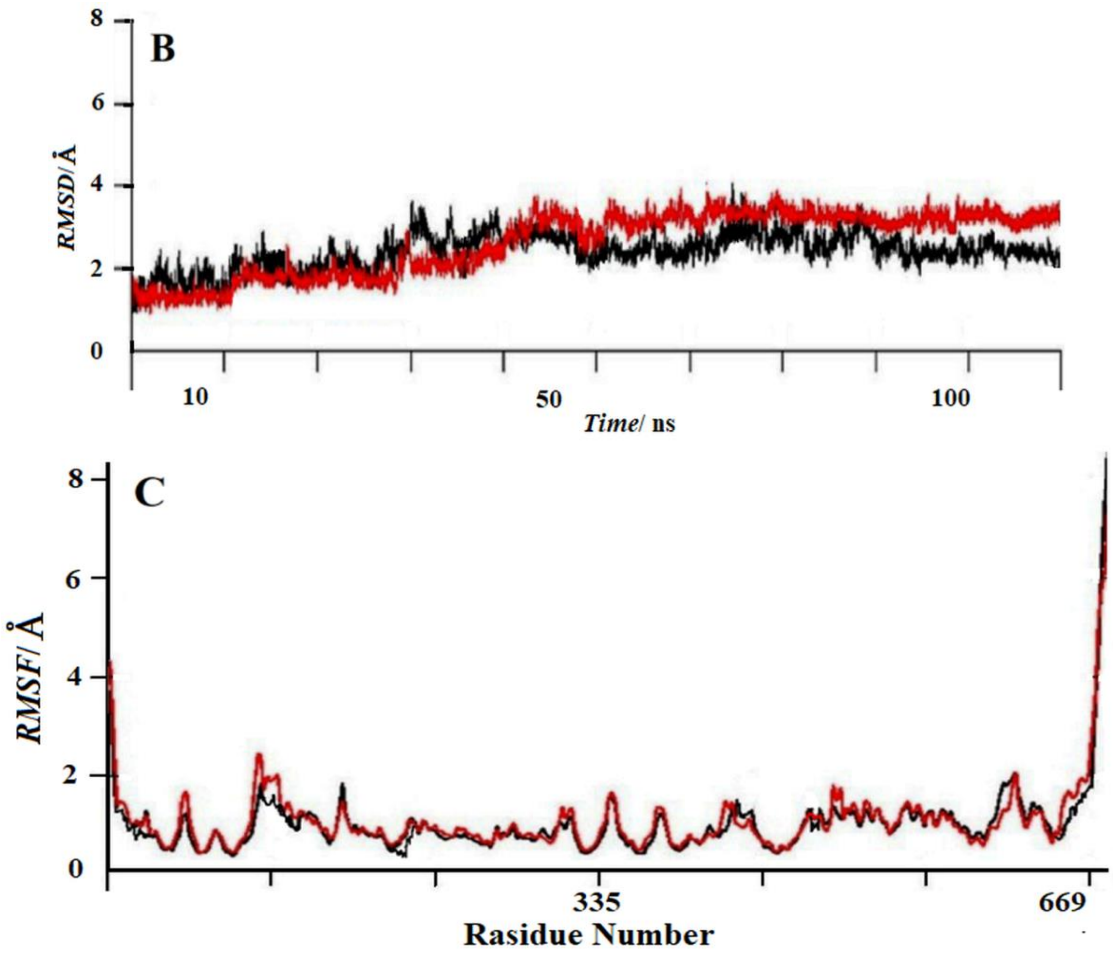

Fig. 4. Molecular Dynamics study of 7BZ5 with the considered chemical: (a) *RMSD* and (b) *RMSF* comparison between single protein and docked complex. The red line indicates single protein and black line indicates docked complex.

Conclusion:

In summary the efficacy of the novel Cu(II) complex, [{Diaquo(3,5-dinitrobenzoato-κ^1O^1)(1,10-phenanthroline-κ^2N^1:N^{10})}copper(II)] 3,5-dinitrobenzoate, as a potential anti-COVID agent was explored through molecular docking and simulation studies. These studies revealed a good binding affinity of this complex against SARS-CoV2 spike protein. Interestingly, low GI and good skin permeation values suggest that the complex may be a good candidate for injection against Covid-19. However, further *in vivo* and *in vitro* studies are required to ascertain the proper binding mechanism of the complex with the virus spike protein as well as to understand the drug behavior of novel Cu(II) complex.

Supplementary Material

Additional data are available electronically at the pages of journal website: http//www.shd-pub.org.rs/index.php/JSCS/index, or from the corresponding author on request. Further crystal details (CCDC 1487797) can be obtained free of charge from the Cambridge Crystallographic Data Center via www.ccdc. cam.ac.uk/data_request/cif.

Acknowledgements. The authors would like to acknowledge Departmental Special Assistance Scheme under the University Grants Commission, New Delhi (SAP-DRS-III, No. 540/12/DRS/2013) & University of North Bengal, Department of Biotechnology, Govt. of West Bengal for financial and instrumental support. The authors also acknowledge "Centre de Diffractometrie Henri Longchambon" at Universite Claude Bernard Lyon 1 for Single crystal X-ray diffraction studies.

Conflict of Interest:

The authors declared that they have no conflict of interest.

References:

[1] A. S. Fauci, H. C. Lane, R. R. Redfield, *N. Engl. J. Med.* **382** (2020) 1268. (https://doi.org0.1056/NEJMe2002387)

[2] H. A. Rothan, S. N. Byrareddy, *J. Autoimmun.* **109** (2020) 102433 (httpds://doi: 10.1016/j.jaut.2020.10243)

[3] WHO Coronavirus update (COVID-19) Dashboard https://www.worldometers.info/coronavirus/country/india/(accessed on 29.11.2020)

[4] R. K. Guy, R. S. DiPaola, F. Romanelli, R. E. Dutch, *Science*. **368 (**2020) 829 (https://doi.org/10.1126/science.abb9332)

[5] P. Gautret, J. –C. Lagier, P. Parola, V. T. Hoang, L. Meddeb, M. Mailhe, B. Doudier, J. Courjon, V. Giordanengo, V. E. Vieira, H. T. Dupont, S. Honor_e, P. Colson, E. Chabri_ere, B. La Scola, J. –M. Rolain, P. Brouqui, D. Raoult, *Int. J. Antimicrob. Agents.* **56** (2020) 105949. (https://doi.org/10.1016/j.ijantimicag.2020.105949)

[6] C. Huang, Y. Wang, X. Li, L. Ren, J. Zhao, Y. Hu, L. Zhang, G. Fan, J. Xu, X. Gu, Z.C. Cheng, T. Yu, J. Xia, Y. Wei, W. Wu, X. Xie, W. Yin, H. Li, M. Liu, Y. Xiao, H. Gao, L. Guo, J. Xie, G. Wang, R. Jiang, Z. Gao, Q. Jin, J. Wang, B. Cao, *Lancet.* **395** (2020) 497 (https://doi.org/10.1016/S0140-6736(20)30183-5)

[7] F. Wu, S. Zhao, B. Yu, Y.-M. Chen, W. Wang, Z.-G. Song, Y. Hu, Z.-W. Tao, J.-H. Tian, Y.-Y. Pei, M.-L. Yuan, Y.-L. Zhang, F.-H. Dai, Y. Liu, Q.-M. Wang, J.-J. Zheng, L. Xu, E. C. Holmes, Y.-Z. Zhang, *Nature*. **579** (2020) 265 (https://doi.org/10.1038/s41586-020-2008-3)

[8] W. Tai, L. He, X. Zhang, J. Pu, D. Voronin, S. Jiang, Y. Zhou, L. Du, *Cell. Mol. Immunol.* **17 (**2020) 613 (https://doi.org/10.1038/s41423-020-0400-4)

[9] S. K. Sinha, A. Shakya, S. K. Prasad, S. Singh, N. S. Gurav, R. S. Prasad, S. S. Gurav, *J. Biomol. Struct. Dyn.* **39(9)** 2020 3244 (https://doi.org/10.1080/07391102.2020.1762741)

[10] G. A. Gyebi, O. B. Ogunro, A. P. Adegunloye, O. M. Ogunyemi, S. O. Afolabi, *J. Biomol. Struct. Dyn.* **39(9)** 2020 3396 (https://doi.org/10.1080/07391102.2020.1764868)

[11] Z. Jin, X. Du, Y. Xu, Y. Deng, M. Liu, Y. Zhao, Y. Duan, *Nature*. **582** (2020) 289. (https://doi.org/10.1038/s41586-020-2223-y)

[12] L. Mittal, A. Kumari, M. Srivastava, M. Singh, S. Asthana, *J. Biomol. Struct. Dyn.* **39** (2020) 1 (https://doi.org/10.1080/07391102.2020.1768151)

[13] J. M. Sanders, M. L. Monogue, T. Z. Jodlowski, J. B. Cutrell, *JAMA*, 323 (2020) 1824 (https://doi.org/10.1001/jama.2020.6019)

[14] S. K. Enmozhi, K. Raja, I. Sebastine, J. Joseph, *J. Biomol. Struct. Dyn.* 39 (2020) 3092. (https://doi.org/10.1080/07391102.2020.1760136)

[15] M. A. Hendaus, *J. Biomol. Struct. Dyn.* **39** (2020) 3787. (https://doi.org/10.1080/07391102.2020.1767691)
[16] H. Li, Y. Zhou, M. Zhang, H. Wang, Q. Zhao, J. Liu, *Antimicrob. Agents Chemother.* **64(6)** (2020) 1. (https://doi.org/10.1128/AAC.00483-20)
[17] C. Duncan, A. R. White, *Metallomics*, **4** (2012) 127. (https://doi.org/10.1039/C2MT00174H)
[18] J. Gallagher, C. B. Chen, C. Q. Pan, D. M. Perrin, Y. M. Cho, D. S. Sigman, *Bioconjugate chem.* **7** (1996) 413. (https://doi.org/10.1021/bc960028t)
[19] E. K. Efthimiadou, M. E. Katsarou, A. Karaliota, G. Psomas, *J. Inorg. Biochem.* **102** (2008) 910 (https://doi.org/10.1155/2013/306385)
[20] J. E. Weder, C. T. Dillon, T. W. Hambley, B. J. Kennedy, P. A. Lay, J.R. Biffin, H. L. Regtop, N. M. Davies, *Coord. Chem. Rev.* **232**, (2002) 95 (https://doi.org/10.1016/S0010-8545(02)00086-3)
[21] J. O. Noyce, H. Michels, C. W. Keevil, *Appl. Environ. Microbiol.* **73** (2007) 2748 (https://doi.org/10.1128/AEM/.01139-06)
[22] F. Lebon, N. Boggetto, M. Ledecq, F. Durant, Z. Benatallah, S. Sicsic, R. Lapouyade, O. Kahn, A. Mouithys-Mickalad, G. D. Dupont, M. R. Ravaux, *Biochem. Pharmacol.* **63** (2002) 1863 (https:// doi: 10.1016/s0006-2952(02)00918-8)
[23] CRYSALISPRO, Oxford Diffraction Ltd. Version 1.171.33.46 (release 27-08-2009 CrysAlis171.NET), Empirical absorption correction using spherical harmonics, implemented in SCALE3 ABSPACK scaling algorithm
[24] J. D. Meulenaar, H. Tompa, *Acta Crystallogr., Sect. A.* **19** (1964) 1014 (https://doi.org/10.1107/S0365110X65004802)
[25] A. Altomare, M. C. Burla, M. Camalli, G. L. Cascarano, C. Giacovazzo, A. Guagliardi, A. G. G. Moliterni, G. Polidori and R. Spagna *J. Appl. Cryst.* **32** (1999) 115 (https://doi.org/10.1107/S0021889898007717)
[26] D. J. Watkin, C. K. Prout, J. R. Carruthers, P. W. Betteridge, R. I. Cooper, *Cristals* **11** (2000) Chemical Crystallography Laboratory, Oxford, UK, (1999)
[27] R.I. Cooper, A.L. Thompson, D.J. Watkin, *J. Appl. Crystallogr.* **43** (2010) 1100 (https://doi.org/10.1107/S0021889810025598)
[28] A. Kamath, G. Pilet, A. Tamang, B. Sinha, *J. Mol. Struct*. **1199** (2020) 126933 (https://doi.org/10.1016/j.molstruc.2019.126933)
[29] G. M. Morris, R. Huey, W. Lindstrom, M. F. Sanner, R. K. Belew, D. S. Goodsell, A. Olson, *J. Comput. Chem.* **30** (2009) 2785 (https://doi.org/10.1002/jcc.21256)
[30] S. Pronk, S. Páll, R. Schulz, P. Larsson, P. Bjelkmar, R. Apostolov, B. Hess, *Bioinformatics.* **29** (2013) 845 (https://doi.org/10.1093/bioinformatics/btt055)
[31] K. Boussery, F.M. Johan, V. De Voorde, Chapter 31 - Physiological Aspects Determining the Pharmacokinetic Properties of Drugs, The Practice of Medicinal Chemistry. (2008) 637 (https://doi.org/10.1016/B978- 0- 12- 374194- 3.0 0 031-7)
[32] F. Ntie-Kang, L. L. Lifongo, J. A. Mbah, L. C. O. Owono, E. Megnassan, L. M. Mbaze, P.N. Judson, W. Sippl, A. M. N. Efange, *In Silico Pharmacol*. **1** (2013) 12 (https://doi.org/10.1186/2193-9616- 1-12)
[33] Swiss Institute of Bioinformatics. SwissADME (http://www.swissadme.ch/index.php)
[34] A. Daina, O. Michielin, V. Zoete, *Sci. Rep.* **7** (2017) 42717 (https://doi.org/10.1038/srep42717)

[35] R. T. Gephart, N. J. Williams, J. H. Reibenspies, A. S. de Sousa, R.D. Hancock, *Inorg. Chem.* **48 (**2009) 8201 (https://doi.org/10.1021/ic900650d)

[36] M. F. Schettini, G. Wu, T. W. Haton, *Inorg. Chem.* **48** (2009) 11799 (https://doi.org/10.1021/ic9018508)

[37] Di. Sun, N. Zhang, Q.-J. Xu, R.-B. Huang, L.-S. Zheng, *Inorg. Chem. Commun.* **13** (2010) 859 (https://doi.org/10.1016/j.inoche.2010.04.014)

[38] A. W. Addison, N. T. Rao, J. Reedijk, J. van Rijn, G. C. Verschoor, *J. Chem. Soc., Dalton Trans.* **7** (1984) 1349 (https://doi.org/10.1039/DT9840001349)

[39] C. P. Chen, C. C. Chen, C. W. Huang, Y. C. Chang, *Molecules* **23** (2018) 911 (https://doi.org/10.3390/molecules23040911)

[40] H. Kim, H. Park, S. J. Lee, *Sci. Rep.* **7 (**2017) 9613. (https://doi.org/10.1038/s41598-017-10110-w).